Response of soil nitrogen retention to the interactive effects of soil texture, hydrology, and organic matter

Michael J. Castellano[1*], David Bruce Lewis[2], Jason P. Kaye[3]

[1]Department of Agronomy

Iowa State University

Ames, IA 50014

[2]Department of Integrative Biology

University of South Florida

Tampa, FL 33620

[3]Department of Crop and Soil Sciences

The Pennsylvania State University

University Park, PA 16802

*Corresponding author:

castellanomichaelj@gmail.com

Abstract

Advances in nitrogen (N) saturation and retention theories have focused on soil organic matter (SOM) biogeochemistry in the absence of dynamic soil hydrology. Here, we exploit two soil types with contrasting texture that span a hillslope gradient to test hypotheses that suggest N saturation symptoms are regulated by the interactive effects of soil texture, organic matter, and hydrology on N retention capacity (maximum pool size) and N retention kinetics (N retention rate). Down the hillslope gradient, soil solution nitrate (NO_3) concentrations sampled with lysimeters increased while $^{15}NO_3$-N retention decreased. Landscape location (upland, hillslope, and toeslope) and soil type interacted to affect soil solution NO_3 concentrations so that the downslope increase in NO_3 was greater in a sandy vs. silty soil. These patterns manifest despite a downslope increase in soil organic carbon (C) and C/N ratios. A positive correlation between saturated hydraulic conductivity and soil solution NO_3 sampled in zero tension lysimeters during precipitation events suggested that high hydraulic conductivity promotes periodic rapid NO_3 transport at rates that exceed retention kinetics. The downslope increase in soil solution NO_3 in spite of a concomitant increase in SOC and C/N ratios provides an important contrast with previous N saturation research that highlights negative correlations between SOM C/N ratios and NO_3 concentrations, and suggests NO_3 transport along connected hillslope flowpaths may overwhelm stoichiometric sinks for inorganic N retention in SOM. Our results reveal important gaps in N retention theory based on SOM biogeochemistry alone, and demonstrate how coupled biogeochemical and hydrologic models can improve predictions of N saturation, particularly when considering periodic advective NO_3 transport in the vadose zone. We show that in coarse-textured soils, low capacity for protection of SOM-N by association with fine mineral particles

interacts with rapid hydrologic flushing of NO_3 to enhance the expression of ecosystem N saturation symptoms.

1. Introduction

Fossil fuel combustion and agricultural activities have increased atmospheric nitrogen (N) deposition. Terrestrial N deposition can lead to symptoms of ecosystem N saturation including soil acidification, increasing nitrate (NO_3) concentrations, vegetation mortality, and N loss to atmospheric and aquatic environments [*Aber et al.*, 1989]. However, the expression of N saturation symptoms can be highly variable among ecosystems despite similar N input. Some ecosystems express N saturation symptoms after small, short-term N additions [*Pregitzer et al.*, 2004] while other ecosystems efficiently retain large N additions in soil organic matter (SOM) sinks that resist mineralization [*Kaye et al.*, 2002; *Magill et al.*, 2000].

Given similar N inputs, ecosystems vary in how quickly they express N saturation symptoms due to either variation in maximum N sink size (capacity), or variation in the rate at which inorganic N can be retained (kinetics) [*Lovett and Goodale*, 2011]. Thus, there are two routes to N saturation: capacity saturation (N sinks are filled) and kinetic saturation (N input rate exceeds N retention rate). The dominant ecosystem N sink is SOM and most N saturation symptoms are manifest as a result of kinetic N saturation [*Schlesinger*, 2009].

Although it is well known that biological *and* hydrological processes account for variation in N saturation and retention [*Gu and Riley*, 2010; *Maggi et al.*, 2008], most empirical research exclusively focuses on SOM biogeochemistry *or* watershed hydrology [*Mitchell*, 2001]. As a result, ecosystem N saturation has been characterized by a variety of biological and hydrological symptoms. Biological studies focus on surface SOM properties and the biological demand for N;

biological symptoms of N saturation include low SOM C/N ratios, low efficiency of inorganic N retention in SOM, and low microbial N demand in addition to high net nitrification, high soil solution NO_3 concentrations, and high NO_3 leaching [*Emmett*, 2007; *Lewis and Kaye*, 2011; *Lovett et al.*, 2002; *Zogg et al.*, 2000]. In contrast, hydrological studies focus on the temporal pattern and magnitude of ecosystem NO_3 export at soil pedon and watershed scales [*Dittman et al.*, 2007; *van Verseveld et al.*, 2008]. Large NO_3 export with little seasonal variation is symptomatic of capacity N saturation (N sinks are filled) [*Lovett et al.*, 2000]. Alternatively, increased NO_3 concentrations and export during periodic episodes of high water flow is symptomatic of kinetic N saturation (N transport rates exceed N retention kinetics). In these situations, rapid soil water flow can overwhelm the kinetics of biological NO_3 immobilization in SOM sinks [*Evans et al.*, 2008]. Evidence of this process includes observations of NO_3 flushing, a pattern which is manifest during intense precipitation events and characterized by rapid NO_3 transport from nutrient-rich surface soils through subsoils to watershed discharge [*Creed and Band*, 1998; *Pionke et al.*, 1996; *van Verseveld et al.*, 2008].

We hypothesize that effects of soil texture on SOM stabilization and hydrology interact to regulate biological N demand and hydrological N transport. The capacity to retain inorganic N inputs in SOM sinks is affected by soil texture [*Castellano et al.*, 2012; *Kaye et al.*, 2002]. Physico-chemical association of SOM with fine mineral particles (silt and clay) can protect N from microbial mineralization thereby maintaining high microbial N demand [*Sollins et al.*, 1996]. Lower fine particle surface area in sandy soils limits SOM protection from mineralization thereby decreasing the potential for inorganic N transfer to and retention in SOM [*Castellano et al.*, 2012; *Six et al.*, 2002]. However, inorganic N inputs must be microbially transformed to organic N compounds before they can be retained in SOM pools that resist mineralization

[*Norton and Firestone*, 1996; *Zogg et al.*, 2000]. Rapid hydrological inputs of inorganic N in coarse-textured soils with high hydraulic conductivity could overwhelm microbial immobilization processes, limiting the retention of inorganic N in SOM [*Evans et al.*, 2008]. Consistent with this hypothesis, N retention in sandy soils is often low, particularly during rainfall events [*Lajtha et al.*, 1995; *Pregitzer et al.*, 2004].

As ecosystem N inputs accumulate, soil texture also affects the pattern of N retention over time. Sandy soils have less SOM stabilization capacity than silty soils and the kinetics of N retention decline as capacity fills [*Castellano et al.*, 2012; *Stewart et al.*, 2007]. Hydrological flowpaths could generate a similar pattern in space. As dissolved C and N inputs accumulate down flowpaths, down-flowpath N sinks could approach capacity more quickly and exhibit slower retention kinetics than up-flowpath N sinks. Thus, hydrological processes could hasten the expression of biological N saturation symptoms by leading to a relatively rapid accumulation of N inputs in down-flowpath N sinks.

Recent numerical models of ecosystem N dynamics incorporate interactions between microbial processes and advective transport [*Gu and Riley*, 2010; *Maggi et al.*, 2008]. However, models have limited ability to accurately characterize large N fluxes during short periods of time such as the rapid N transport that occurs during intense precipitation events. Moreover, empirical data regarding interactions among microbial and hydrological processes are scarce. Here, we link SOM and hydrological processes to explain interactions between capacity and kinetic N retention controls on N saturation symptoms along hillslope flowpaths in two adjacent soil types with fine and coarse texture. The two soil types supported a mature hardwood forest that had no significant differences in dominant vegetation or throughfall N deposition. We hypothesized that soils with coarse texture would exhibit more symptoms of N saturation including higher soil

solution inorganic N concentrations and lower inorganic N retention in SOM. We further hypothesized that these N saturation symptoms would increase downslope due to accumulation of dissolved N inputs in SOM sinks.

2. Methods

2.1 Site Description

The ~ 0.5 ha study site is located Abingdon, MD USA (39º27'05"N, 76º16'23"W). The site is part of the Chesapeake Bay, MD National Oceanic and Atmospheric Association National Estuarine Research Reserve. Mean annual temperature is 12.0 ˚C. Mean annual precipitation is 1164 mm. Vegetation at the site is a mix of *Liquidambar styraciflua, Liriodendron tulipifera,* and *Quercus* spp. Tree ring analyses indicate that many individuals of the dominant tree species (*L. styraciflua.*) are >110 years old (unpublished data, 2009). According to the United States Department of Agriculture Natural Resources Conservation Service (USDA NRCS), the study site contains two soil orders and three soil series: two silty Ultisols (Joppa and Elsinboro series) and a sandy Entisol (Evesboro series). We could not distinguish the two Ultisols in the field, and they are sampled as one soil type for this study. The soils are derived from quartz parent materials, however, additional mineralogical data is not available. The site is part of a small catchment that spans upland to floodplain. The three soil series span upland to floodplain, perpendicular to the catchment drainage. The NE end of the catchment contains the Ultisols and the SW end of the catchment contains the Entisol. The catchment gradient spans ~40 m from upland-to-floodplain with ~20% slope (Figure 1). Ground-penetrating radar surveys conducted by the USDA NRCS indicated that the soils are ~1 m deep and underlain by an aquitard that influences water flow laterally downslope (unpublished data, 2009). The aquitard was visually

confirmed to be a lithified paleosol with low hydraulic conductivity likely dating to the Cretaceous (T. White, pers. comm.). The paleosol effect on water flow was apparent at the floodplain intersection of the paleosol and soil surface where water regularly seeped (supporting material).

2.2 Sampling Approach

We established 8 transects that spanned upland to floodplain, perpendicular to catchment drainage (Figure 1). Four transects were located in the Ultisols and four transects were located in the Entisol. Each transect included an upland, hillslope and toeslope sampling location (12 sample locations in each soil order). Hillslope locations were midway between the upland and toeslope locations. We sampled soil solution and measured inorganic N retention at the 3 transect locations. In 2007 and 2008, we installed Prenart^{TM} quartz tension lysimeters (Denmark) at transect locations. At all upland and hillslope locations, tension lysimeters were inserted at the interface between the A and B soil horizons (12-15 cm) as well as at the bottom of the B soil horizon (~85-100 cm below the soil surface). At the toeslope locations, tension lysimeters were only inserted at the A/B soil horizon interface (shallow depth) on three of the four transects in each soil type (6 of 8 total toeslope locations) due to equipment limitations. We also installed polyvinyl chloride zero tension lysimeters (ZTL) at the interface between the A and B soil horizons at all upland and hillslope locations (to correspond with shallow tension lysimeters). We did not install ZTLs at toeslope locations because the water table reached the A horizon during intense precipitation events, confounding our ability to sample water moving vertically and laterally down the hillslope. Nevertheless, all toeslope locations were above water seeps and exhibited no redoximorphic features or alluvial discontinuities. Tension lysimeters were fabricated from a porous quartz material; a vacuum (-70 kPa) was placed on the lysimeter

for ~18 h during which a sample was collected. These samples were not collected during rain events and thus sampled soil solution that was not moving rapidly. In contrast, ZTLs 'catch' water that is advectively transported into the collection area which was 30.0 x 9.6 cm. Our observations suggest this advective transport of soil water was limited to periods of intense or large rainfall.

The lysimeters were allowed a 14-20 month equilibration period during which they were sampled every 2-4 weeks. These samples were discarded. From 1 October 2008 to 5 November 2009 (after the equilibration period), we sampled all tension lysimeters every 1-4 weeks, with more frequent sampling during times when all lysimeters were collecting samples (Feb-June). We sampled all ZTLs after intense precipitation events. Our first lysimeter samples were collected in December 2008 due to dry soil conditions during October-November that did not produce samples. All replicate tension lysimeters yielded samples through mid-July and all replicate ZTLs yielded samples through August (supporting material). Some replicate lysimeters yielded samples through November 2009. Throughfall was also sampled at each transect location (N = 24). Lysimeter and throughfall solution was kept on ice in a cooler for < 4 h, frozen, thawed, filtered (Whatman 1), and analyzed for NH_4-N and NO_3-N concentrations. Throughfall and tension lysimeter water samples were also analyzed for oxygen isotope ratios in H_2O ($\delta^{18}O$).

In August 2008 we extracted 5 replicate A horizon soil cores at all upland, hillslope, and toeslope transect locations (24 total locations) and 5 replicate B horizon soil cores at the upland and hillslope transect locations (16 of the 24 locations) using a 15 cm deep x 5 cm diameter soil core sampler and butyrate liners (i.e., 200 soil cores sampled in butyrate liners). Sampling of B horizons at the 8 locations at the bottom of the flowpaths was prevented due to deep B horizon soils (> 30 cm) that exhibited redoximorphic features. In a few locations, the A horizon was <15

cm deep; in these situations we removed the B horizon portion from the soil core prior to analyses. Soil from the 200 cores was used for analyses of bulk density, soil texture, soil organic C (SOC), soil organic N (SON), C/N ratio, 2M KCl extractable NH_4 and NO_3 pool sizes, and 3 d transfer of $^{15}NH_4$-N and $^{15}NO_3$-N to soil pools that were not extractable with 2M KCl.

On the August 2008 sampling date, using the 5 intact soil cores collected at each transect location, we injected two cores with $^{15}NH_4Cl$, two cores with $K^{15}NO_3$, and the fifth core was reserved to determine ^{15}N natural abundance. Soil cores from the A horizon were injected with 0.75 mg of 70.4% APE $^{15}NH_4Cl$-N and 0.5 mg of 60.2% APE $K^{15}NO_3$-N while B horizon soil cores were injected with 0.6 mg of 70.4% APE $^{15}NH_4Cl$-N and 0.4 mg of 60.2% APE $K^{15}NO_3$-N. Masses of NH_4 and NO_3 applications were selected to limit increases in background concentrations while permitting detection of the ^{15}N tracer in relatively large SOM-N pools. On average, these ^{15}N additions increased the A horizon NH_4 pool by 17%, the B horizon NH_4 pool by 26%, the A horizon NO_3 pool by 26%, and the B horizon NO_3 pool by 35%. All N applications were delivered in injections of deionized water that totaled 5 mL of solution per soil core and increased soil moisture by ~1.7%. Cores were capped at both ends; the top cap was perforated to allow for gas exchange. Fifteen minutes after injection, the ambient core, one $^{15}NH_4Cl$-injected soil core and one $K^{15}NO_3$- injected soil core were extracted for NH_4 and NO_3 by reciprocal shaking for 2 h in a 2 M KCl solution at a m/v ratio of 1:5 (soil:KCl). After shaking, the solution was filtered (pre-leached Whatman 1) for determination of NH_4-N and NO_3–N on a flow injection spectrophotometer. Initial NH_4-N and NO_3-N pools (mass N/mass dry soil < 2mm) were determined from the mean value of these three soil cores. The remaining $^{15}NH_4Cl$-injected soil core and $K^{15}NO_3$- injected soil core were left in the field to incubate for 3d, and then NH_4-N and NO_3-N extracted using the above procedure. The mass of $^{15}NH_4$-N and

$^{15}NO_3$-N that remained in the residual extracted soil after 3d was measured; we assume this represented N that was immobilized in SOM during the 3d incubation. We calculated the 3 d transfer of $^{15}NH_4$-N and $^{15}NO_3$-N to SOM as a fraction of the mean initial NH_4-N and NO_3-N pools that were labeled with ^{15}N and determined from the cores extracted at 15 min.

In August 2008, we sampled one 26.5 cm deep x 9 cm diameter soil core at upland and hillslope transect locations (N = 16 total cores) for laboratory analysis of saturated hydraulic conductivity (Ks). Samples were collected to test hypotheses regarding ZTL N concentrations and thus were not collected at toeslope locations where ZTLs were absent. Samples were refrigerated at 4^{o}C for approximately one week for lab analyses. The constant head method was used to determine Ks (Klute and Dirksen 1986) with minor modifications as suggested by Walker (2007). Prior to analysis, the cores were saturated in a solution of de-aired 0.005 M calcium sulfate to minimize soil flocculation. Air was removed from the solution by bubbling with He through an aquarium aerator. We determined Ks with Darcy's equation (1).

$$Ks = QL / A(H_2-H_1) \quad (1)$$

Where:

Ks = Saturated hydraulic conductivity (cm/s)

Q = Volume of water discharged per time (cm^3/s)

L = Length of core (cm)

A = Cross sectional area of inner sampling region (cm^2)

(H_2-H_1) = Hydraulic head difference (cm)

Dissolved inorganic N concentrations in lysimeter solutions and throughfall were determined with microplate spectrophotometry. Solid soil sample C and N concentrations and N

isotope ratios were determined with an elemental analyzer interfaced to an isotope ratio mass spectrometer. Oxygen isotope ratios were determined from throughfall and lysimeter solutions with a laser water isotope analyzer. All isotope analyses were conducted at the University of California Stable Isotope Facility (Davis, CA). Total soil C and N are the means of the five soil core samples from each sample location. Soil texture was determined with the method presented by [*Kettler et al.*, 2001] on one composite sample derived from the five soil cores at each location. Bulk density was measured for each core using the mass of dry soil (< 2 mm) and the volume of sample.

2.3 Data Analysis

Because we were interested in the effects of soil order, landscape locations and soil depth on inorganic N concentrations, we calculated the mean inorganic N concentrations for each of the three lysimeter types (shallow and deep tension lysimeters and shallow ZTLs) across sample dates when all lysimeters collected soil solution. All shallow tension lysimeters yielded soil solution on 13 sampling occasions, all deep tension lysimeters yielded soil solution on 12 occasions, and all ZTLs yielded soil solution on 10 occasions (supporting material). Therefore, to derive the spatial mean, inorganic N concentrations were first averaged over time within location (among the above sample occasions) and then averaged across replicate locations (for each soil type, N = 4 for upland and hillslope; N = 3 for toeslope).

Data were analyzed with regression and analysis of variance (ANOVA). The ability of SOM properties and Ks to explain variation in lysimeter N concentrations and inorganic N retention were explored with regression analyses. Heteroscedastic data were log10 transformed. Independently, SOM properties, tension lysimeter and ZTL inorganic N concentrations, 3 d

inorganic N retention in unextractable pools, and Ks were analyzed as dependent variables with 3-way ANOVA. Lysimeter data were analyzed with an unbalanced 3-way ANOVA because we lacked toeslope lysimeters in one of the three transects in each soil type. Soil order and landscape location were analyzed as main plots and soil depth was treated as a split plot. The interaction between soil depth and landscape location was not analyzed due to the lack of depth sampling at the toeslope location. Soil hydrology (Ks) and ZTL data were analyzed with 2-way ANOVA due to a lack of sampling at two soil depths. Soil order and landscape location were treated as main plots.

Oxygen isotope data were used to estimate the transit time (mean residence time) of water sampled in A and B soil horizon tension lysimeters [*Dewalle et al.*, 1997; *Maloszewski et al.*, 1983]. A sine wave model was fitted to annual fluctuations in $\delta^{18}O$ of H_2O in throughfall inputs and lysimeter solutions:

$$\delta^{18}O = X + A\,[\cos(ct - \theta)] \quad (2)$$

where $\delta^{18}O$ is the predicted O isotope ratio in ‰, X is the annual mean $\delta^{18}O$ in ‰, A is the annual amplitude of $\delta^{18}O$ in ‰, c is the radial frequency of $\delta^{18}O$ in radians (0.017214 radians day^{-1}), t is the time in days after the first water sample (15 December 2008) and θ is the peak annual $\delta^{18}O$ in radians. Subsequently, the dampening of the annual $\delta^{18}O$ amplitude in the lysimeter solution sine wave models compared to the annual $\delta^{18}O$ amplitude in the throughfall solution sine wave model can be used to estimate transit time as:

$$T = c^{-1}[A_{z2}/A_{z1})^{-2}\text{-}1]^{0.5} \quad (3)$$

where *T* is transit time, *c* is defined above, A_{z2} is the amplitude of the lysimeter soil solution model and A_{z1} is the amplitude of the throughfall sine wave model. Because this method only provides a rough estimate of transit time and all lysimeters did not collect water throughout the one-year period required for these analyses, we did not calculate unique transit times for each individual lysimeter. Instead, we fitted models to $\delta^{18}O$ data that was pooled among all replicate lysimeters across soil types for each landscape and soil depth location (N=8 lysimeters in A and B soil horizons at upland and hillslope locations; N = 6 A horizon lysimeters at toeslope locations). Although we would expect transit time to differ among the soil types due to differences in texture, this modeling approach is not expected to be sufficiently sensitive to accurately characterize small differences in transit time [*Dewalle et al.*, 1997]. Accordingly, we used this approach to explore potential differences in H_2O transit time among the upland, hillslope and toeslope landscape positions as well as among the A and B soil horizons.

3. Results

Sand content was higher in the Entisol while silt and clay contents were higher in the Ultisols (Tables 1 and 2). Bulk density did not vary predictably with soil properties or landscape location (data not shown). Accordingly, we report soil C and N per mass of dry soil (< 2 mm). Total SOC and SON were well correlated ($R = 0.98$; $p < 0.0001$). Soil type did not have a significant effect on SOC or SON; however, C/N ratio was lower in the sandy Entisols (Tables 1 and 2, Figure 2). Landscape location had a significant effect on SOC, SON, and C/N ratio (Table 2); all increased downslope (Figure 2).

Inorganic N concentrations in tension lysimeter samples were greater in the sandy Entisols and increased downslope (Table 2 and Figure 3). Significant interactions between soil

type and landscape location indicated that the downslope increase in tension lysimeter NH_4-N and NO_3-N concentrations was greater in sandy Entisols compared to silty Ultisols (Table 2 and Figure 3). Concentrations of NH_4-N in ZTLs did not differ among soil types or landscape locations. However, concentrations of NO_3-N in ZTLs were greater in the Entisol and increased downslope (Table 2 and Figure 3).

Retention of $^{15}NH_4$-N in SOM during the 3 d in situ incubation was only affected by soil horizon (Table 2). A greater fraction of the initial NH_4-N pool was retained in B horizons versus A horizons (Figure 4). In contrast, retention of $^{15}NO_3$-N during the 3 d incubation was affected by landscape location and soil horizon (Table 2). A greater fraction of initial NO_3-N pools was retained in B horizons and NO_3-N retention decreased downslope in both horizons (Figure 4).

Regression analyses between SOM properties, soil solution inorganic N concentrations, and ^{15}N retention only revealed significant negative correlations between A horizon $^{15}NH_4$-N retention and A horizon SON ($R = -0.70$, $p = 0.0002$) and SOC ($R = -0.68$, $p = 0.0010$); SOM C/N ratios were not correlated with soil solution inorganic N concentrations or inorganic N retention. However, sand and silt contents were correlated with A horizon $^{15}NH_4$-N retention, soil solution NO_3-N concentrations in the A horizon, and Ks. In all cases correlations with sand were stronger and in the opposite direction of correlations with silt; accordingly we display correlations with sand only. Variation in clay contents was low (Table 1) and not correlated with any variables. Retention of $^{15}NH_4$-N in A horizon soils was negatively linearly correlated with sand (Figure 5) and positively linearly correlated with silt ($R = 0.51$, $p = 0.0106$). Soil solution NO_3-N concentrations in A horizon tension lysimeters and ZTLs were positively correlated with sand (Figure 5) and negatively correlated with silt ($R = -0.55$, $p = 0.0086$ for tension lysimeters and $R = -0.60$, $p = 0.0141$ for ZTLs). Similarly, Ks was positively correlated with sand (Figure

6) and negatively correlated with silt ($R = -0.76$, $p < 0.0006$). NO_3-N concentrations in ZTLs were positively correlated with Ks (Figure 6). All correlations with Ks required log10 transformation to reduce heteroscedasticity. Soil type and landscape location had a significant effect on Ks (Table 2); the sandy Entisol had higher Ks than the silty Ultisols and Ks was greater at the hillslope location compared to the upland location (Table 2 and Figure 6).

Transit time estimates of soil solutions sampled in A horizon tension lysimeters increased downslope from 75 days at the upland location to 108 days at the hillslope location and 179 days at the toeslope location. Transit time estimates for B horizon soil solutions were 276 days for the upland location and 237 days for the toeslope location (Table 3 and Figure S2).

4. Discussion

4.1 Site Hydrology

Soil hydrology and texture data indicate that downslope water transport occurs through lateral flow within soil horizons as well as vertical flow through soil horizons. The downslope increase in transit time estimates of A horizon soil solution sampled with tension lysimeters (Table 3) is consistent with some downslope lateral flow within the A horizon. Abrupt changes in soil properties at horizon interfaces can promote lateral flow [*Lin and Zhou*, 2008] and our lysimeters were placed at the interface of the A and B soil horizons. Steep slopes (20%; Figure 1) may further promote lateral flow. The downslope increase in transit time could not be attributed to lower hydraulic conductivity at downslope locations because Ks increased downslope (Tables 1 and 2). Although we found no downslope difference in volumetric water contents (unpub. data), this finding may be the result of downslope changes in Ks and texture (Tables 1 and 2). This lack of difference does, however, indicate that differences in SOM decomposition are not

responsible for downslope increases in SOC, SON, and NO_3. Moreover, the concomitant downslope increase in C/N ratios and NO_3 concentrations suggests NO_3 is not be produced locally, but transported from upslope. Together, these data suggest the presence of connected lateral flowpaths through hillslope surface soils. Nevertheless, vertical flow through soil horizons to the paleosol with low hydraulic conductivity and subsequent downslope travel is also likely important. Evidence for this process includes visible water flow at the toeslope seep where the paleosol interfaces with the surface soil (supporting material).

4.2 Nitrogen Dynamics along the Slope

Our results suggest hydrological flowpaths and soil type interact to modulate N saturation symptoms including soil solution NO_3 concentrations and NO_3 retention in SOM. Soil solution NO_3 concentrations increased downslope while $^{15}NO_3$-N retention decreased downslope (Figures 2 and 3). The downslope increase in soil solution NO_3 in ZTL samples, which incorporated the effects of periodic advective transport, was greater in the sandy Entisol with greater Ks than the silty Ultisols (Table 2 and Figure 2). In contrast, we found relatively few effects of soil type, hillslope location, or their interaction on measures of N saturation that did not incorporate advective processes; there was no effect of soil type on $^{15}NH_4$ or $^{15}NO_3$ retention in SOM (Table 2 and Figure 4). Accordingly, the intense periodic advective NO_3 transport that was captured by ZTL sampling appears to be an important contributor to downslope and subsoil biogeochemistry. Across all sampling locations, higher NO_3 concentrations in ZTLs compared to tension lysimeters indicate that biological N demand is not completely saturated at any sampling location, affirming the dual importance of periodic transport and biological N immobilization. However, higher Ks, lower $^{15}NH_4$-N retention, and higher NO_3 concentrations in sandy soils

(Figures 5 and 6) indicate differences in hydrology and N retention kinetics account for greater variation in N dynamics than biological demand.

Our results provide important contrasts with previous N saturation research that has focused on biological demand and demonstrated positive correlations among SOC, C/N ratios and N retention as well as negative correlations among SOC, C/N ratios and soil solution NO_3 [*Emmett et al.*, 1998; *Evans et al.*, 2006; *Lovett et al.*, 2002]. At our site, the downslope increase in soil solution NO_3 concentrations and decrease in NO_3 retention occurred concomitant with a downslope increase in SOC and C/N ratios (Table 2 and Figures 2, 3, and 4). We suggest inorganic N inputs via lateral hillslope flowpaths may overwhelm positive effects of increasing SOC and C/N ratios on downslope inorganic N retention. The established relationship between C/N ratios and N saturation symptoms is highly variable within the range of C/N ratios at our site [*Ross et al.*, 2009] and soil hydrology may be one factor contributing to that variation.

Several processes could have contributed to increasing downslope SOC and SON concentrations including microclimate, soil physical properties, and an accumulation of dissolved C and N inputs from upslope. However, research focusing on vertical soil water flowpaths has determined that dissolved organic matter (DOM) transport from surface soils is an important source of subsoil SOM accumulation [*Marin-Spiotta et al.*, 2011; *Sanderman and Amundson*, 2008]. Similarly, significant portions of surface soil inorganic N production can be retained in subsoils after transformation to SON [*Dittman et al.*, 2007; *Huygens et al.*, 2008]. Soil solution data from tension lysimeters confirm subsoils are an important sink for inorganic N at our site: the mean NO_3-N decrease from A to B soil horizons was 50% (Figure 2). Further, our ^{15}N retention measurements suggest that the decrease can be explained by NO_3-N transfer to insoluble SOM (Figure 3). Although we cannot determine the importance of downslope lateral

flow in the A horizon, the downslope increase in SOC, SON and NO_3 concentrations is consistent with lateral hydrological transport downslope.

Consistent with SOM saturation theory [*Six et al.*, 2002], increasing downslope SOC and SON concentrations could be the result of long-term DOM inputs from upslope locations that concomitantly increase downslope SOM pools and decrease downslope N retention. Although the downslope decrease in $^{15}NO_3$ retention and increase in SON concentrations may appear inconsistent, the efficiency of dissolved organic C and N retention in insoluble SOM can decrease with increasing SOM-C and SOM-N concentrations [*Castellano et al.*, 2012; *Stewart et al.*, 2007] and most inorganic N retention in insoluble SOM occurs after biological transformation to dissolved organic N and subsequent adsorption to solid particles [*Norton and Firestone*, 1996; *Sollins et al.*, 1996; *Zogg et al.*, 2000].

4.3 Nitrogen Dynamics in Contrasting Soil Types

There is no consistent relationship among soil texture and N cycling. For example, sand content, N mineralization, and dissolved NO_3 fluxes have been reported to be positively, negatively, or not correlated [*Bechtold and Naiman*, 2006; *Cote et al.*, 2000; *Giardina et al.*, 2001; *Gu and Riley*, 2010; *Pastor et al.*, 1984; *Reich et al.*, 1997]. Positive correlations between sand, N mineralization, and N fluxes may be the result of lower potential N stabilization in silt and clay associated SOM. Negative correlations may be the result of soil texture effects on water content. Sandy soils typically have low water holding capacity, and water content is a key control on C and N dynamics [*Castellano et al.*, 2011]. Moreover, relationships among soil texture and N cycling are often confounded by differences in vegetation biochemistry [*Mueller et al.*, 2012; *Pastor et al.*, 1984; *Reich et al.*, 1997], a variable which was controlled at our site.

Recent research suggests that inconsistent relationships among soil texture and N cycling may be reconciled by focusing on the capacity for silt and clay particles to stabilize SOM [*Castellano et al.*, 2012]. Soils with large capacity for SOM stabilization in silt + clay fractions, regardless of texture, may exhibit high inorganic N retention and low N mineralization. The capacity for SOM stabilization in silt + clay fractions is a function of silt + clay contents as well as cumulative OM inputs [*Hassink*, 1997]. The unoccupied capacity for SOM stabilization by silt + clay these particles can be described as the SOM or SOC 'saturation deficit' [*Stewart et al.*, 2007].

At our site, the negative relationships among sand, SOM, and $^{15}NH_4$-N retention in SOM, coupled with the positive correlation between sand content and soil solution NO_3 concentrations (Figure 6), suggest sandy soils have lower N retention kinetics that result in lower microbial N demand and higher NO_3 concentrations. During intense precipitation events that produced rapid advective soil solution transport, high Ks in sandy soils appears to promote flushing of NO_3 that has accumulated due to low retention (Figures 5 and 6). Positive correlations among Ks and ZTL NO_3 concentrations suggest that increasing soil solution transport rates decrease NO_3 retention in SOM. These data are consistent with NO_3 flushing concepts [*Creed and Band*, 1998; *van Verseveld et al.*, 2008] and contribute to the biological understanding of NO_3 flushing processes.

5. Conclusions

Explaining why ecosystems vary in how quickly they reach N saturation remains an important challenge. Recent conceptual models suggest that the time to onset of N saturation symptoms is a function of N uptake capacity and kinetics [*Lovett and Goodale*, 2011]. Our results suggest that the rate at which an ecosystem retains N (kinetics), the rate at which an

ecosystem transports N, and the total amount of N it can retain (capacity), are functions of SOM properties and hydraulic conductivity, which are regulated in turn by soil texture. We demonstrate that a downslope increase in NO_3 concentrations is coincident with a downslope decrease in inorganic N retention capacity (Figures 2 and 3). We hypothesize that downslope transport of dissolved C and N contributes to this observation. If widespread, this pattern could help to account for variability in watershed NO_3 export. Indeed, a recent study of nine watersheds in the northeastern United States demonstrated that a topographic index (tangent of upslope area/slope) was positively correlated with NO_3 export while the ability of potential nitrification rates to explain variation in watershed NO_3 export was significantly improved when data were limited to downslope soils near the stream and watershed outlet [*Ross et al.*, 2012].

As N inputs accumulate, soil texture can impact the kinetics and capacity of N retention. In ecosystems with sandy soils, N retention is often low [*Lajtha et al.*, 1995; *Pregitzer et al.*, 2004]. We link this observation to hydrological and physicochemical mechanisms that affect N retention kinetics and capacity. The potential rate of dissolved N transport (Ks) was positively correlated with soil solution NO_3 concentrations (Figure 4) while NO_3 retention was lower and NO_3 concentrations were higher in soils with low capacity for physico-chemical SOM-N protection by association with silt and clay particles (Figure 2 and 3).

The effects of soil texture on N retention may be difficult to observe in ecosystems with low SOM or rapid biomass accumulation rates because N sinks should efficiently retain large N inputs [*Castellano et al.*, 2012; *Vitousek and Reiners*, 1975]. However, as the capacity for N retention decreases, so should the kinetics of N retention. These results may help to explain variation in the NO_3 flushing pattern, which is not universally observed [*Hill et al.*, 1999]. In watersheds where the NO_3 flushing pattern is absent, N retention capacity should be relatively

large with rapid kinetics. Alternatively, in watersheds where NO_3 flushing is manifest as a result of rapid NO_3 transport from surface soils, N retention capacity should be low, thereby decreasing N retention kinetics that can mitigate NO_3 loss during rapid soil water flow.

Advances in N saturation and retention theories have focused on surface soil N biogeochemistry in the absence of dynamic soil hydrology. Our results reveal important gaps in N retention theory based on soil biogeochemistry alone, and demonstrate how microbial and hydrological processes can interact to affect N dynamics. Recent numerical models of N dynamics that incorporate microbial processes as well as advective transport offer an excellent framework to interpret the relative importance of biological and hydrological controls on the expression of N saturation symptoms [*Gu and Riley*, 2010; *Maggi et al.*, 2008]. These models distinguish between kinetic and capacity N saturation processes and have the potential to explain patterns in our data that are coincident with N inputs, hydrology and SOM stabilization capacity. In soils with coarse texture, low capacity for physico-chemical SOM-N protection by association with silt and clay particles (capacity saturation) may feedback with rapid advective N transport (kinetic saturation) to hasten the expression of ecosystem N saturation symptoms.

Literature Cited

Dennis Lock provided statistical advice and programming. This project was funded by NSF (DEB Dissertation Improvement Grant-090999) and NOAA (National Estuarine Research Reserve) to MJC. JPK was funded by NSF DEB 0816668. MJC was funded by USDA (National Needs 2005-38420-15774).

Literature Cited

Aber, J., K. Nadelhoffer, P. Steudler, and J. M. Melillo (1989), Nitrogen saturation in northern forest ecosystems., *BioScience*, *39*, 378–386.

Bechtold, S. J., and R. J. Naiman (2006), Soil texture and nitrogen mineralization potential across a riparian toposequence in a semi-arid savanna, *Soil Biology and Biochemistry*, *38*(6), 1325–1333, doi:10.1016/j.soilbio.2005.09.028. [online] Available from: http://linkinghub.elsevier.com/retrieve/pii/S003807170500369X (Accessed 29 December 2011)

Castellano, M. J., J. P. Kaye, H. Lin, and J. P. Schmidt (2012), Linking Carbon Saturation Concepts to Nitrogen Saturation and Retention, *Ecosystems*, doi:10.1007/s10021-011-9501-3. [online] Available from: http://www.springerlink.com/index/10.1007/s10021-011-9501-3 (Accessed 28 November 2011)

Castellano, M. J., J. P. Schmidt, J. P. Kaye, C. Walker, C. B. Graham, H. Lin, and C. Dell (2011), Hydrological controls on heterotrophic soil respiration across an agricultural landscape, *Geoderma*, *16*, 273–280, doi:10.1016/j.geoderma.2011.01.020.

Cote, L., S. Brown, D. Pare, F. J, and B. J (2000), Dynamics of carbon and nitrogen mineralization in relation to stand type , stand age and soil texture in the boreal mixedwood, *Soil Biology and Biochemistry*, *32*, 1079–1090.

Creed, I. F., and L. E. Band (1998), Export of nitrogen from catchments within a temperate forest : Evidence for a unifying mechanism regulated by variable source area dynamics, *Water Resources*, *34*(11), 3105–3120.

Dewalle, D. R., P. J. Edwards, B. R. Swistock, R. Aravena, and R. J. Drimmie (1997), Seasonal isotope hydrology of three appalachian forest catchments, *Journal of Hydrology*, *11*(April 1996), 1895–1906.

Dittman, J. a, C. T. Driscoll, P. M. Groffman, and T. J. Fahey (2007), Dynamics of nitrogen and dissolved organic carbon at the Hubbard brook experimental forest., *Ecology*, *88*(5), 1153–66.

Emmett, B. A. (2007), Nitrogen Saturation of Terrestrial Ecosystems: Some Recent Findings and Their Implications for Our Conceptual Framework, *Water, Air, & Soil Pollution: Focus*, *7*(1-3), 99–109, doi:10.1007/s11267-006-9103-9. [online] Available from: http://www.springerlink.com/index/10.1007/s11267-006-9103-9 (Accessed 13 July 2011)

Emmett, B. A., D. Boxman, M. Bredemeier, P. Gundersen, O. J. Kjønaas, F. Moldan, P. Schleppi, A. Tietema, and R. F. Wright (1998), Predicting the Effects of Atmospheric Nitrogen Deposition in Conifer Stands : Evidence from the NITREX Ecosystem-Scale Experiments, *Ecosystems*, *1*, 352–360.

Evans, C. D. et al. (2006), Evidence that Soil Carbon Pool Determines Susceptibility of Semi-Natural Ecosystems to Elevated Nitrogen Leaching, *Ecosystems*, *9*(3), 453–462, doi:10.1007/s10021-006-0051-z. [online] Available from: http://www.springerlink.com/index/10.1007/s10021-006-0051-z (Accessed 29 December 2011)

Evans, C. D., D. Norris, N. Ostle, H. Grant, E. C. Rowe, C. J. Curtis, and B. Reynolds (2008), Rapid immobilisation and leaching of wet-deposited nitrate in upland organic soils., *Environmental pollution (Barking, Essex : 1987)*, *156*(3), 636–43, doi:10.1016/j.envpol.2008.06.019. [online] Available from: http://www.ncbi.nlm.nih.gov/pubmed/18653264 (Accessed 6 December 2011)

Giardina, C. P., M. G. Ryan, R. M. Hubbard, D. Binkley, and F. E. For (2001), Tree Species and Soil Textural Controls on Carbon and Nitrogen Mineralization Rates, *Soil Science Society of America Journal*, *65*, 1272–1279.

Gu, C., and W. J. Riley (2010), Combined effects of short term rainfall patterns and soil texture on soil nitrogen cycling - a modeling analysis., *Journal of contaminant hydrology*, *112*(1-4), 141–54, doi:10.1016/j.jconhyd.2009.12.003. [online] Available from: http://www.ncbi.nlm.nih.gov/pubmed/20116129 (Accessed 13 September 2012)

Hassink, J. (1997), The capacity of soils to preserve organic C and N by their association with clay and silt particles, *Plant and Soil*, *191*, 77–87.

Hill, A. R., W. A. Kemp, J. M. Buttle, and G. D. (1999), Nitrogen chemistry of subsurface storm runoff on forested Canadian Shield hillslopes, *Water Resources*, *35*(3), 811–821.

Huygens, D., P. Boeckx, P. Templer, L. Paulino, O. Van Cleemput, C. Oyarzún, C. Müller, and R. Godoy (2008), Mechanisms for retention of bioavailable nitrogen in volcanic rainforest soils, *Nature Geoscience*, *1*(8), 543–548, doi:10.1038/ngeo252. [online] Available from: http://www.nature.com/doifinder/10.1038/ngeo252 (Accessed 11 July 2011)

Kaye, J., J. Barrett, and I. Burke (2002), Stable Nitrogen and Carbon Pools in Grassland Soils of Variable Texture and Carbon Content, *Ecosystems*, *5*, 461–471, doi:10.1007/s10021-002-142-4.

Kettler, T. A., J. W. Doran, and T. L. Gilbert (2001), Simplified Method for Soil Particle-Size Determination to Accompany Soil-Quality Analyses, *Soil Science Society of America Journal*, *65*, 849–852.

Lajtha, K., B. Seely, and I. Valiela (1995), Retention and leaching losses of atmospherically-derived nitrogen in the aggrading coastal watershed of Waquoit Bay, MA, *Biogeochemistry*, (Howarth 1988), 33–54.

Lewis, D. B., and J. P. Kaye (2011), Inorganic nitrogen immobilization in live and sterile soil of old-growth conifer and hardwood forests: implications for ecosystem nitrogen retention, *Biogeochemistry*, doi:10.1007/s10533-011-9627-6. [online] Available from: http://www.springerlink.com/index/10.1007/s10533-011-9627-6 (Accessed 16 September 2011)

Lin, H., and X. Zhou (2008), Evidence of subsurface preferential flow using soil hydrologic monitoring in the Shale Hills catchment, *European Journal of Soil Science*, *59*(1), 34–49, doi:10.1111/j.1365-2389.2007.00988.x. [online] Available from: http://doi.wiley.com/10.1111/j.1365-2389.2007.00988.x (Accessed 20 August 2012)

Lovett, G. M., and C. L. Goodale (2011), A New Conceptual Model of Nitrogen Saturation Based on Experimental Nitrogen Addition to an Oak Forest, *Ecosystems*, *14*(4), 615–631,

doi:10.1007/s10021-011-9432-z. [online] Available from: http://www.springerlink.com/index/10.1007/s10021-011-9432-z (Accessed 21 August 2011)

Lovett, G. M., K. C. Weathers, and M. a. Arthur (2002), Control of Nitrogen Loss from Forested Watersheds by Soil Carbon:Nitrogen Ratio andTree Species Composition, *Ecosystems*, *5*(7), 712–718, doi:10.1007/s10021-002-0153-1. [online] Available from: http://www.springerlink.com/openurl.asp?genre=article&id=doi:10.1007/s10021-002-0153-1 (Accessed 20 July 2011)

Lovett, G. M., K. C. Weathers, and W. V. Sobczak (2000), NITROGEN SATURATION AND RETENTION IN FORESTED WATERSHEDS OF THE CATSKILL MOUNTAINS , NEW YORK, *Ecological Applications*, *10*(1), 73–84.

Maggi, F., C. Gu, W. J. Riley, G. M. Hornberger, R. T. Venterea, T. Xu, N. Spycher, C. Steefel, N. L. Miller, and C. M. Oldenburg (2008), A mechanistic treatment of the dominant soil nitrogen cycling processes: Model development, testing, and application, *Journal of Geophysical Research*, *113*(G2), 1–13, doi:10.1029/2007JG000578. [online] Available from: http://www.agu.org/pubs/crossref/2008/2007JG000578.shtml (Accessed 17 July 2012)

Magill, A. H., J. D. Aber, G. M. Berntson, W. H. McDowell, K. J. Nadelhoffer, J. M. Melillo, and P. Steudler (2000), Long-Term Nitrogen Additions and Nitrogen Saturation in Two Temperate Forests, *Ecosystems*, *3*(3), 238–253, doi:10.1007/s100210000023. [online] Available from: http://www.springerlink.com/openurl.asp?genre=article&id=doi:10.1007/s100210000023 (Accessed 28 July 2011)

Maloszewski, P., W. Rauert, W. Stichler, and A. Herrmann (1983), Application of flow models in an alpine catchment area using tritium and deuterium data, *Journal of Hydrology*, *66*, 319–330.

Marin-Spiotta, E., O. a. Chadwick, M. Kramer, and M. S. Carbone (2011), Carbon delivery to deep mineral horizons in Hawaiian rain forest soils, *Journal of Geophysical Research*, *116*(G3), 1–14, doi:10.1029/2010JG001587. [online] Available from: http://www.agu.org/pubs/crossref/2011/2010JG001587.shtml (Accessed 5 April 2012)

Mitchell, M. J. (2001), Linkages of nitrate losses in watersheds to hydrological processes, *Hydrological Processes*, *15*(17), 3305–3307, doi:10.1002/hyp.503. [online] Available from: http://doi.wiley.com/10.1002/hyp.503 (Accessed 18 July 2011)

Mueller, K. E., S. E. Hobbie, J. Oleksyn, P. B. Reich, and D. M. Eissenstat (2012), Do evergreen and deciduous trees have different effects on net N mineralization in soil?, *Ecology*, *93*(6), 1463–72. [online] Available from: http://www.ncbi.nlm.nih.gov/pubmed/22834386

Norton, M., and M. K. Firestone (1996), N Dynamics in the rhizosphere of Pinus Ponderosa Seedlings, *Soi Biology and Biochemistry*, *28*(3), 351–362.

Pastor, J., J. D. Aber, C. A. Mcclaugherty, and J. M. Melillo (1984), Aboveground production and N and P cycling along a nitrogen mineralization gradient on Blackhawk Island, Wisconsin, *Ecology*, *65*(1), 256–268.

Pionke, H. B., W. J. Gburek, A. N. Sharpley, and R. R. Schnabel (1996), Flow and nutrient export patterns for an agricultural, *Water Resources*, *32*(6), 1795–1804.

Pregitzer, K. S., D. R. Zak, J. Andrew, J. A. Ashby, and N. W. Macdonald (2004), Chronic nitrate additions dramatically increase the export of carbon and nitrogen from northern hardwood ecosystems, *Biogeochemistry*, *68*, 179–197.

Reich, P., D. Grigal, J. Aber, and G. ST (1997), Nitrogen mineralization and productivity in 50 hardwood and conifer stands on diverse soils, *Ecology*, *78*(2), 335–347.

Ross, D. S., J. B. Shanley, J. L. Campbell, G. B. Lawrence, S. W. Bailey, G. E. Likens, B. C. Wemple, G. Fredriksen, and A. E. Jamison (2012), Spatial patterns of soil nitrification and nitrate export from forested headwaters in the northeastern United States, *Journal of Geophysical Research*, *117*(G1), 1–14, doi:10.1029/2011JG001740. [online] Available from: http://www.agu.org/pubs/crossref/2012/2011JG001740.shtml (Accessed 6 April 2012)

Ross, D. S., B. C. Wemple, A. E. Jamison, G. Fredriksen, J. B. Shanley, G. B. Lawrence, S. W. Bailey, and J. L. Campbell (2009), A Cross-Site Comparison of Factors Influencing Soil Nitrification Rates in Northeastern USA Forested Watersheds, *Ecosystems*, *12*(1), 158–178, doi:10.1007/s10021-008-9214-4. [online] Available from: http://www.springerlink.com/index/10.1007/s10021-008-9214-4 (Accessed 15 December 2011)

Sanderman, J., and R. Amundson (2008), A comparative study of dissolved organic carbon transport and stabilization in California forest and grassland soils, *Biogeochemistry*, *92*(1-2), 41–59, doi:10.1007/s10533-008-9249-9. [online] Available from: http://www.springerlink.com/index/10.1007/s10533-008-9249-9 (Accessed 14 October 2011)

Schlesinger, W. H. (2009), On the fate of anthropogenic nitrogen., *Proceedings of the National Academy of Sciences of the United States of America*, *106*(1), 203–8, doi:10.1073/pnas.0810193105. [online] Available from: http://www.pubmedcentral.nih.gov/articlerender.fcgi?artid=2613040&tool=pmcentrez&rendertype=abstract

Six, J., R. T. Conant, E. A. Paul, and K. Paustian (2002), Stabilization mechanisms of soil organic matter : Implications for C-saturation of soils, *Plant and Soil*, *241*, 155–176.

Sollins, P., P. Homann, and B. A. Caldwell (1996), Stabilization and destabilization of soil organic matter : mechanisms and controls, *Geoderma*, *74*, 65–105.

Stewart, C. E., K. Paustian, R. T. Conant, A. F. Plante, and J. Six (2007), Soil carbon saturation: concept, evidence and evaluation, *Biogeochemistry*, *86*(1), 19–31, doi:10.1007/s10533-007-9140-0. [online] Available from: http://www.springerlink.com/index/10.1007/s10533-007-9140-0 (Accessed 15 June 2011)

van Verseveld, W. J., J. J. McDonnell, and K. Lajtha (2008), A mechanistic assessment of nutrient flushing at the catchment scale, *Journal of Hydrology*, *358*(3-4), 268–287,

doi:10.1016/j.jhydrol.2008.06.009. [online] Available from: http://linkinghub.elsevier.com/retrieve/pii/S0022169408002898 (Accessed 19 October 2011)

Vitousek, P. M., and W. A. Reiners (1975), Ecosystem Succession and Nutrient Retention: A Hypothesis, *Bioscience*, *25*, 376–381.

Zogg, G. P., D. R. Zak, K. S. Pregitzer, and A. J. Burton (2000), Microbial immobilization and the retention of anthropogenic nitrate in a northern hardwood forest, *Ecology*, *81*(7), 1858–1866.

Table 1. Mean values for each soil order, soil horizon and landscape location (N = 4).

Soil Type	Landscape Position	Sand (g kg^{-1} soil)	Silt (g kg^{-1} soil)	Clay (g kg^{-1} soil)	Ks* (cm sec^{-1})	Organic Carbon (g C kg^{-1} soil)	Insoluble Nitrogen (g N kg^{-1} soil)	C/N Ratio	pH
Entisol									
A Horizon	Upland	748	181	71	0.08	34.0	1.8	18.5	3.8
	Hillslope	824	106	70	0.15	35.8	1.8	20	3.7
	Toeslope	825	103	72	-	45.1	2.1	21.2	3.9
B Horizon	Upland	769	134	97	-	7.5	0.5	15.8	4.1
	Hillslope	809	112	79	-	6.8	0.4	17.7	4.0
Ultisols									
A Horizon	Upland	544	329	127	0.02	26.3	1.2	22.3	3.9
	Hillslope	668	232	101	0.08	32.3	1.5	22.6	3.4
	Toeslope	710	192	98	-	52.3	2.2	23.6	3.9
B Horizon	Upland	583	301	116	-	6.6	0.4	16.1	4.0
	Hillslope	646	236	118	-	8.5	0.4	19.9	4.0

*Saturated hydraulic conductivity

Table 2. Data represent probability (P > F) of 3-way ANOVA for the effects of independent factors soil type, soil depth (A vs. B horizon), and landscape location on the dependent factors SOM, Tension Lysimeters N, and Inorganic N retention. Zero tension lysimeters were only installed at the shallow depth in upland and hillslope locations; thus, the results represent 2-way ANOVA with the independent factors soil type and landscape location.

	Analysis of Variance												
Factor	Soil Texture			SOM			Tension Lysimeters		Zero Tension Lysimeters		Inorganic N Retention		Hydrology
	Sand	Silt	Clay	SOC	SON	C/N	NH4-N	NO3-N	NH4-N	NO3-N	NH4-N	NO3-N	Ks
Soil Type	<0.0001	<0.0001	0.0024	0.5464	0.7375	0.0119	0.0006	0.0003	0.9694	0.0023	0.7537	0.2195	0.0200
Location	0.0030	0.0061	0.5121	0.0003	0.0096	0.0186	0.0004	0.0121	0.6905	0.0115	0.1737	<0.0001	0.0051
Soil Type x Location	0.4423	0.5777	0.7229	0.1650	0.2194	0.8640	0.0072	0.0648	0.8903	0.0295	0.4665	0.7181	0.3340
Soil Depth	0.7852	0.5060	0.3123	<0.0001	<0.0001	<0.0001	0.1097	0.0009	-	-	0.0023	0.0100	-
Soil Type x Depth	0.9418	0.8552	0.5416	0.1967	0.0385	0.1276	0.2100	0.0218	-	-	0.1640	0.4661	-

Table 3. Annual $\delta^{18}O$ (‰) characteristics of water sampled from throughfall and tension lysimeters that were used parameterize a soil solution transit time model (see methods Equations 2 and 3). Data are displayed in supplementary materials.

Water Type		Minimum	Maximum	Average	SD*	Amplitude	Transit Time
		$\delta^{18}O$ (‰)					days
Throughfall		-14.1	-2.3	-7.3	2.9	-11.7	-
A Soil Horizon Tension Lysimeter (12-15 cm)	Upland	-11.4	-4.3	-6.5	1.1	-7.2	75
	Hillslope	-9.5	-3.9	-6.5	1.1	-5.6	108
	Toeslope	-8.6	-5.0	-6.6	1.0	-3.6	180
B Soil Horizon Tension Lysimeter (85-100 cm)	Upland	-7.9	-5.5	-6.9	0.6	-2.4	276
	Hillslope	-8.0	-5.2	-6.7	0.5	-2.8	237

*Standard Deviation

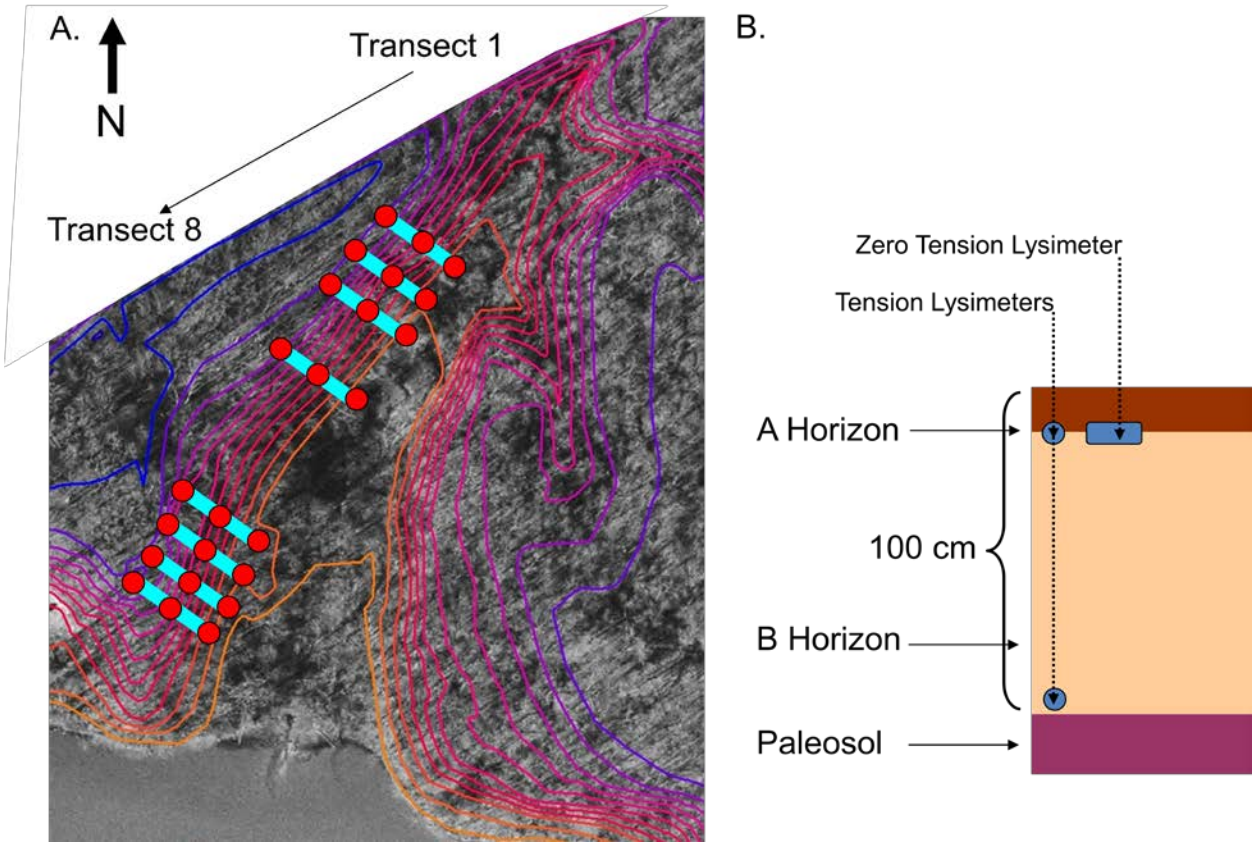

Figure 1. (A) Map of the research location. Contour lines are 1m. Blue lines represent sampling transects (40 m) and red circles represent Upland, Hillslope, and Toeslope sampling locations on each transect. The four northern transect were in silty Ultisol soils. The four southern transects were in a sandy Entisol soil. (B) Sampling approach at Upland and Hillslope transect locations. One tension and one zero tension lysimeter were located at the interface of the A and B soil horizons. A second tension lysimeter was located at the bottom of the B horizon. Toeslope sampling locations did not have zero tension lysimeters or B horizon tension lysimeters and they only had an A horizon tension lysimeter at 3 of 4 transects within each soil type (see Methods).

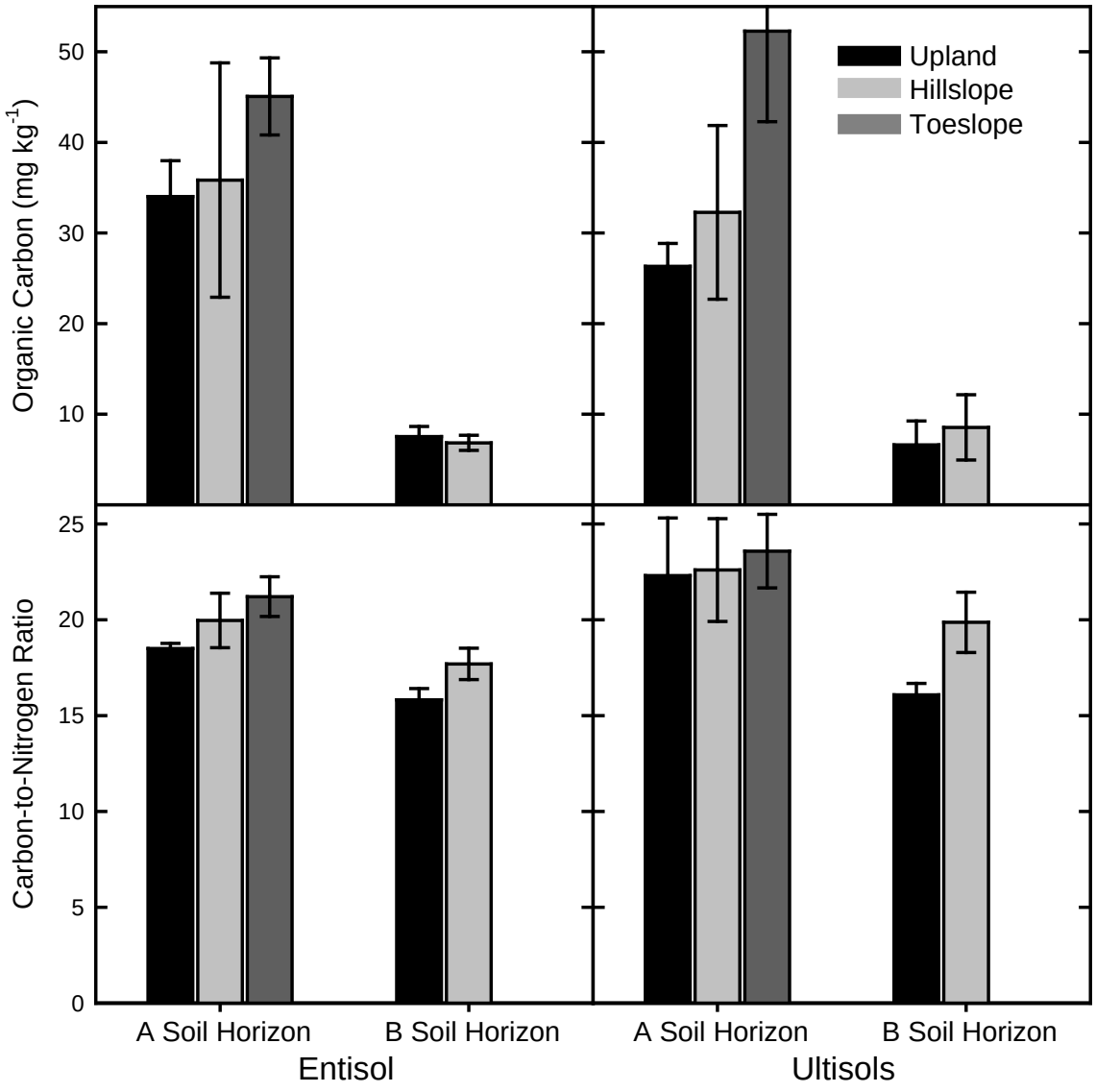

Figure 2. Soil organic matter properties. Data represent the mean and standard error (N=4). Soil carbon-to-nitrogen ratio is reported on a mass basis. See Table 2 for statistics.

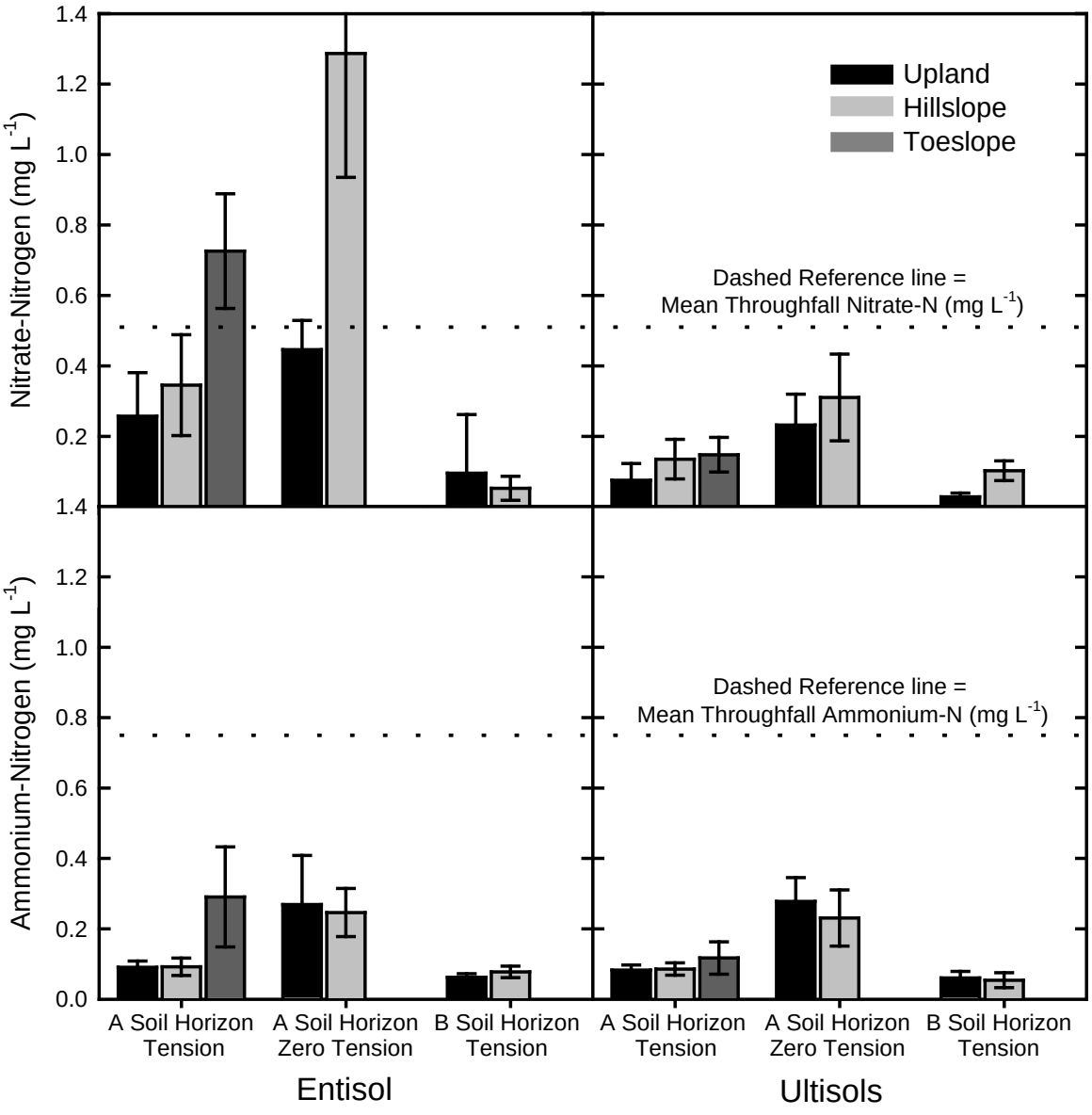

Figure 3. Spatial mean soil solution inorganic nitrogen concentrations and standard error sampled during the 2009 water year (N=4 for Upland and Hillslope locations; N = 3 for toeslope locations). See Table 2 for statistics.

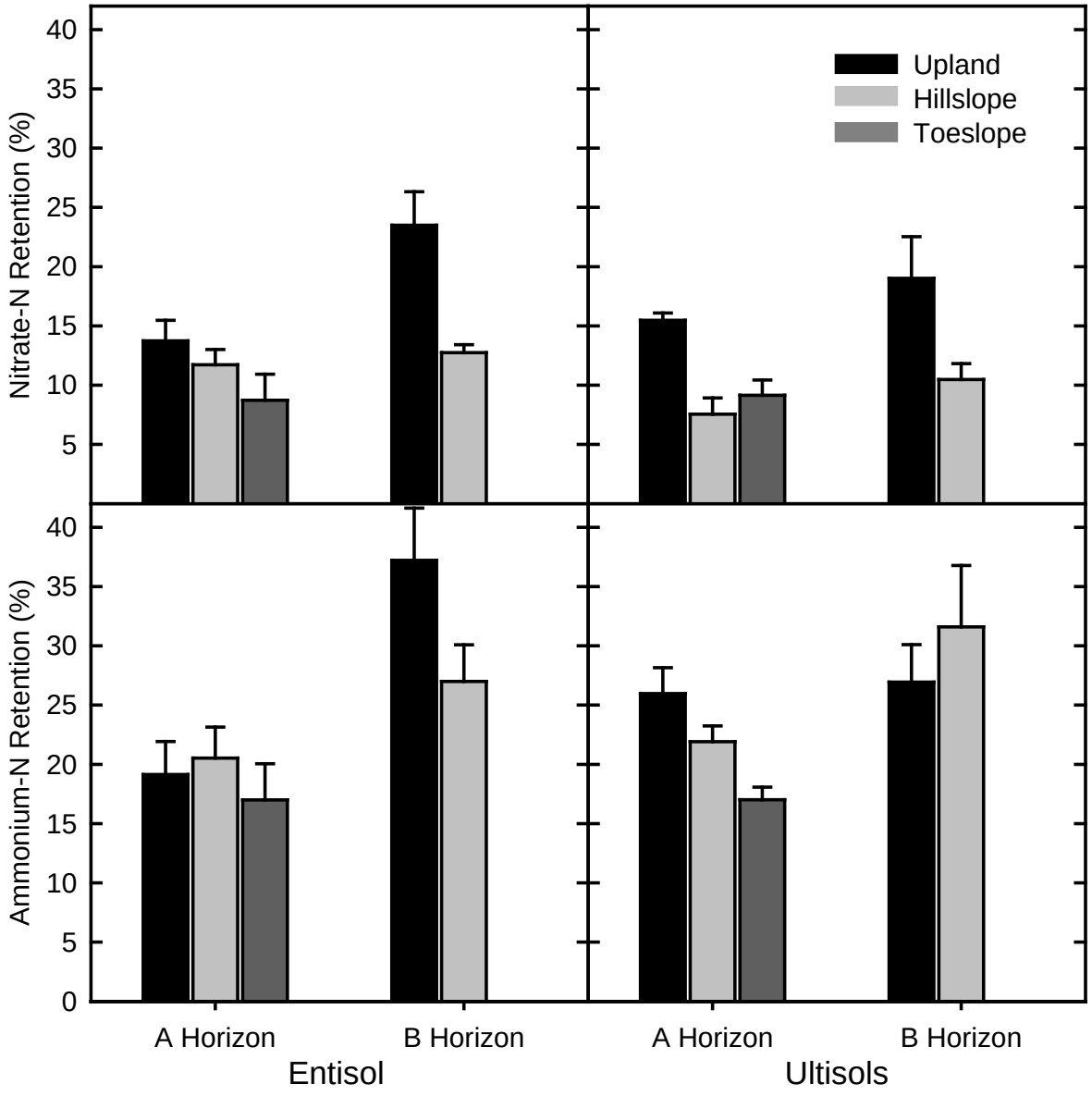

Figure 4. The mean (SE) fraction of ^{15}N-labeled NH_4-N and NO_3-N pools that were retained in soil pools not extractable with 2 M KCl after 3 day in situ incubation; N=4. See Table 2 for statistics.

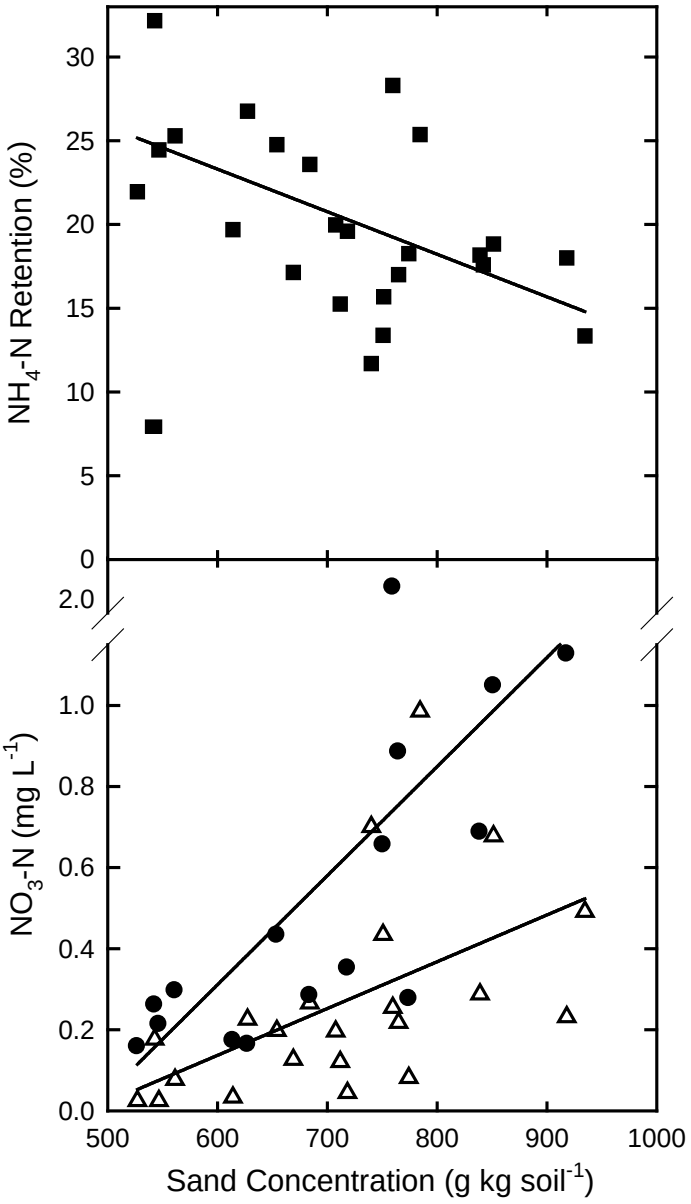

Figure 5. The A soil horizon sand concentration was negatively linearly correlated with A soil horizon NH_4-N retention in insoluble pools during a 3 d in situ incubation (black squares; R = -0.56, p = 0.0444). The A soil horizon sand concentration positively linearly correlated with mean annual zero tension lysimeter NO_3-N concentrations (black circles; R = 0.63, p = 0.0090) and mean annual A horizon tension lysimeter NO_3-N concentration (open triangles; R = 0.53, p = 0.0105).

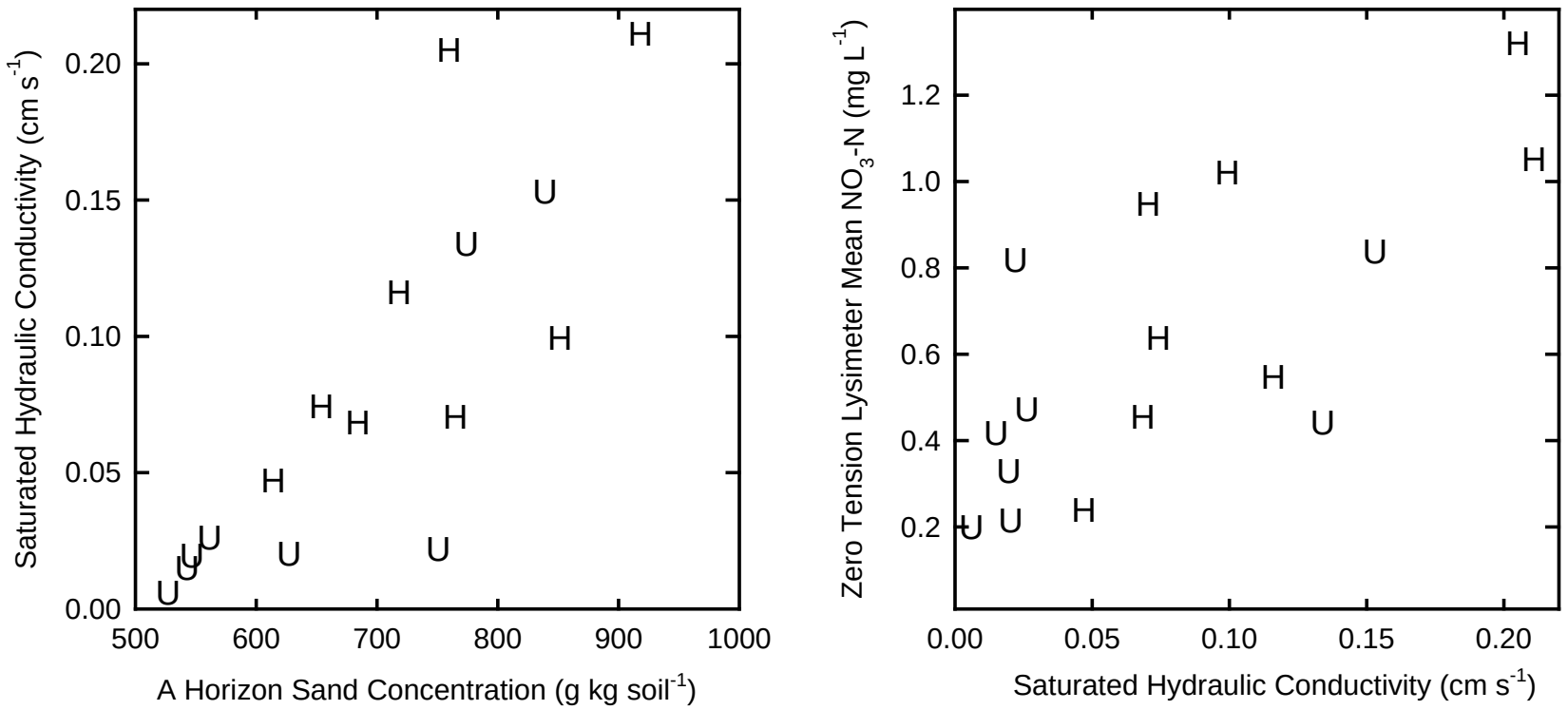

Figure 6. U = Upland; H = Hillslope. Prior to regression analysis, data were log10 transformed to correct for heteroscedasticity. A horizon sand concentration was positively correlated with saturated hydraulic conductivity (R = 0.81, p = 0.0002). Saturated hydraulic conductivity was positively correlated with the spatial mean of zero tension lysimeter NO_3-N concentrations (R = 0.61, p = 0.0116).

Supporting Information

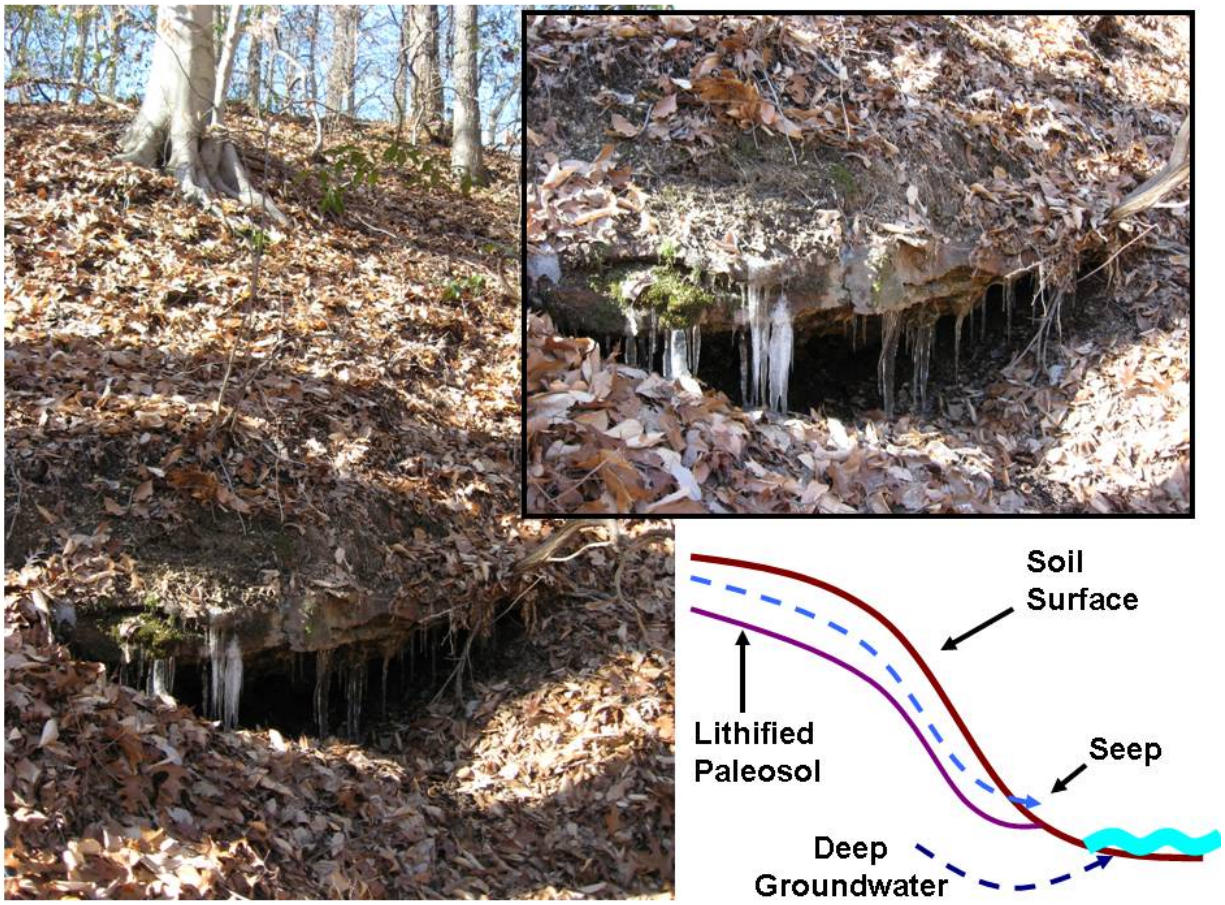

Figure S1. Conceptual understanding of hillslope soil water transport at the research site. All sample locations were above the seep. Ground-penetrating radar surveys conducted by the USDA NRCS indicated that the soil is ~1 m deep and underlain by a stratigraphic unit with low hydraulic conductivity (aquitard) that influences water flow laterally downslope (unpublished data, 2009). The aqutitard is exposed in the above photograph and was confirmed to be a relatively impermeable lithified paleosol likely dating to the Cretaceous (T. White, pers. comm.). The paleosol effect on water flow was apparent at this intersection.

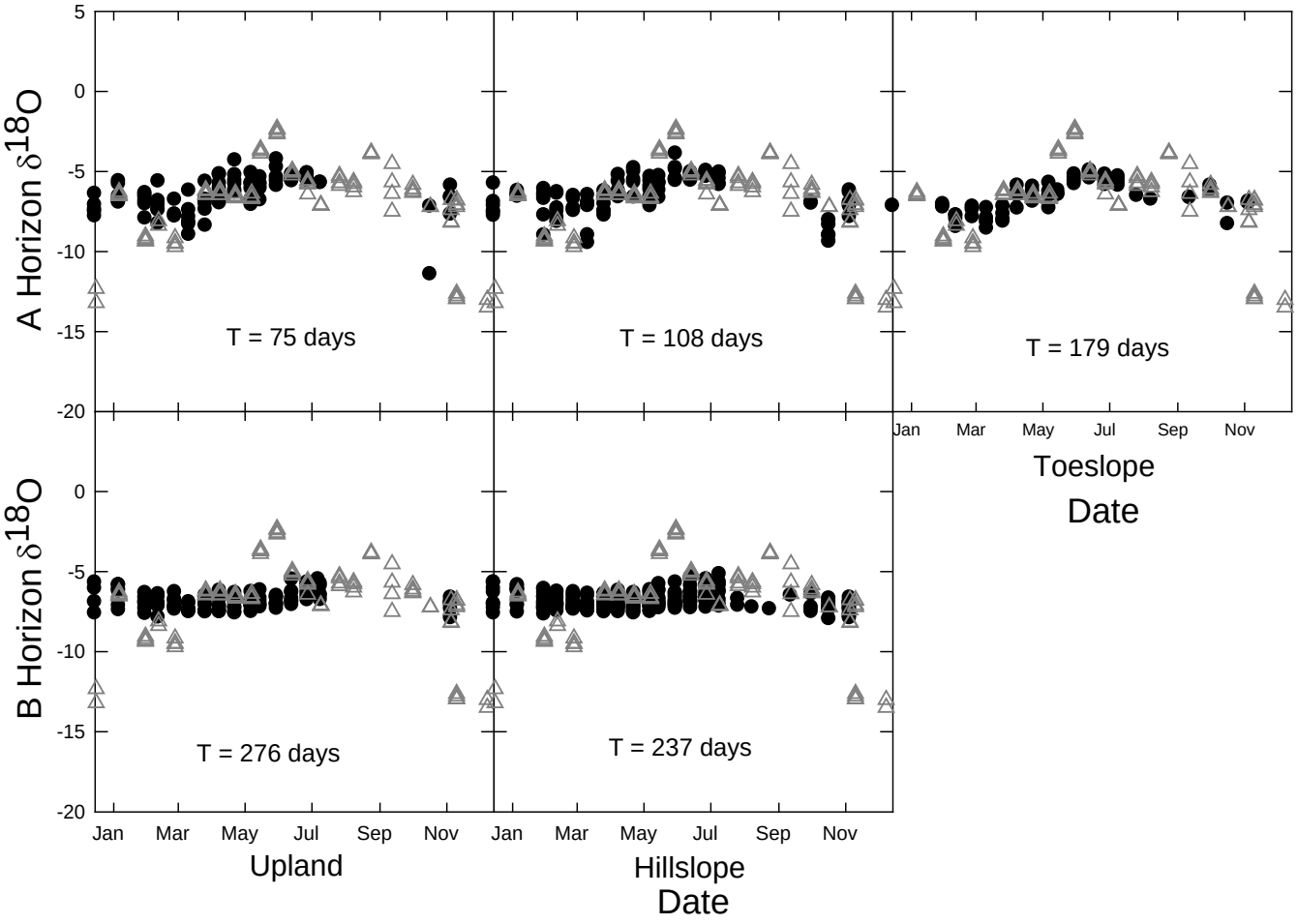

Figure S2.Annual $\delta^{18}O$ (‰) characteristics of water sampled from throughfall (grey open triangles) and tension lysimeters (black circles). T= water transit time in days. The dampening of annual variation in water $\delta^{18}O$ (‰) from throughfall to lysimeter samples was used to estimate water transit time from inputs (throughfall) to lysimeter locations (see methods and Table 3). Throughfall data from all sampling locations was pooled, thus throughfall data in all panels are identical and displayed for reference purposes.

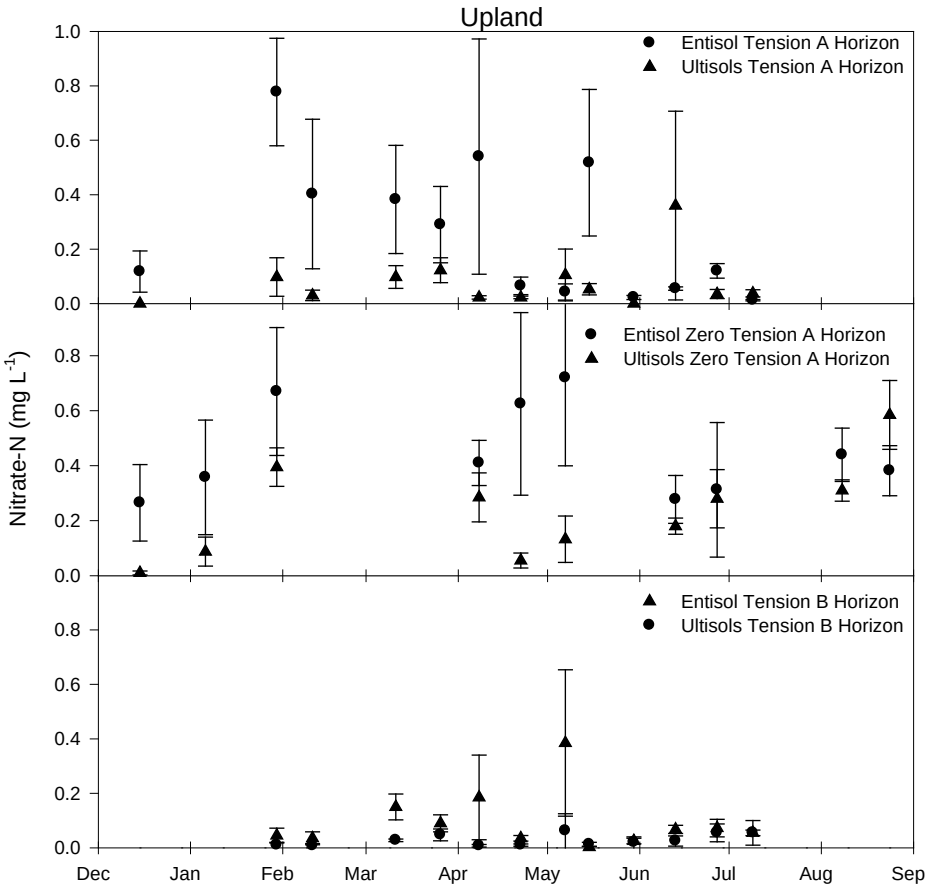

Figure S3. Temporal pattern of nitrate-N concentrations sampled in Entisol and Ultisol soil orders at upland landscape locations with tension and zero tension lysimeters. For each soil order the mean and standard error for is displayed for each sample date (N = 4).

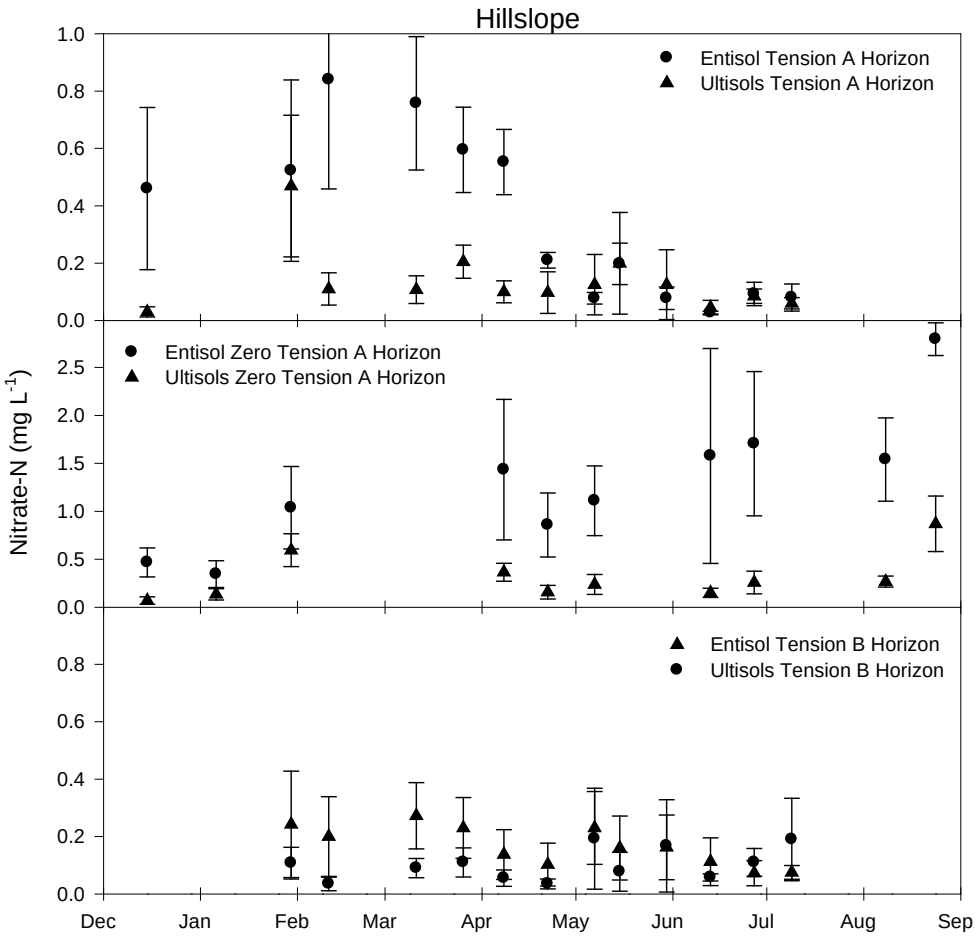

Figure S4. Temporal pattern of nitrate-N concentrations sampled in Entisol and Ultisol soil orders at hillslope landscape locations with tension and zero tension lysimeters. For each soil order the mean and standard error for is displayed for each sample date (N = 4).

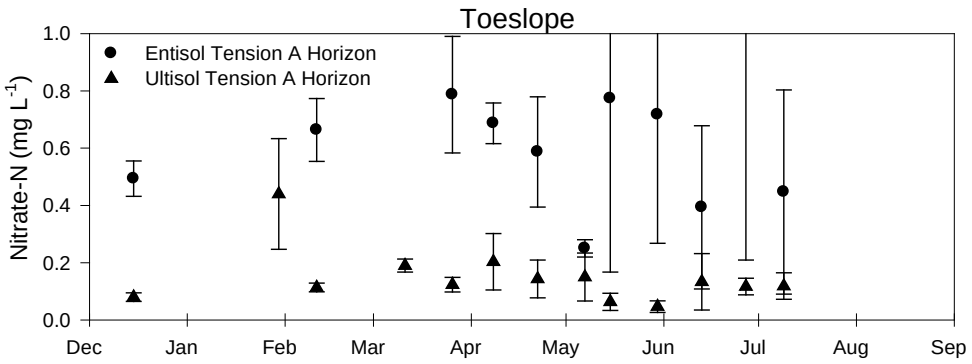

Figure S5. Temporal pattern of nitrate-N concentrations sampled in Entisol and Ultisol soil orders at toeslope landscape locations with tension and zero tension lysimeters. For each soil order the mean and standard error for is displayed for each sample date (N = 3).

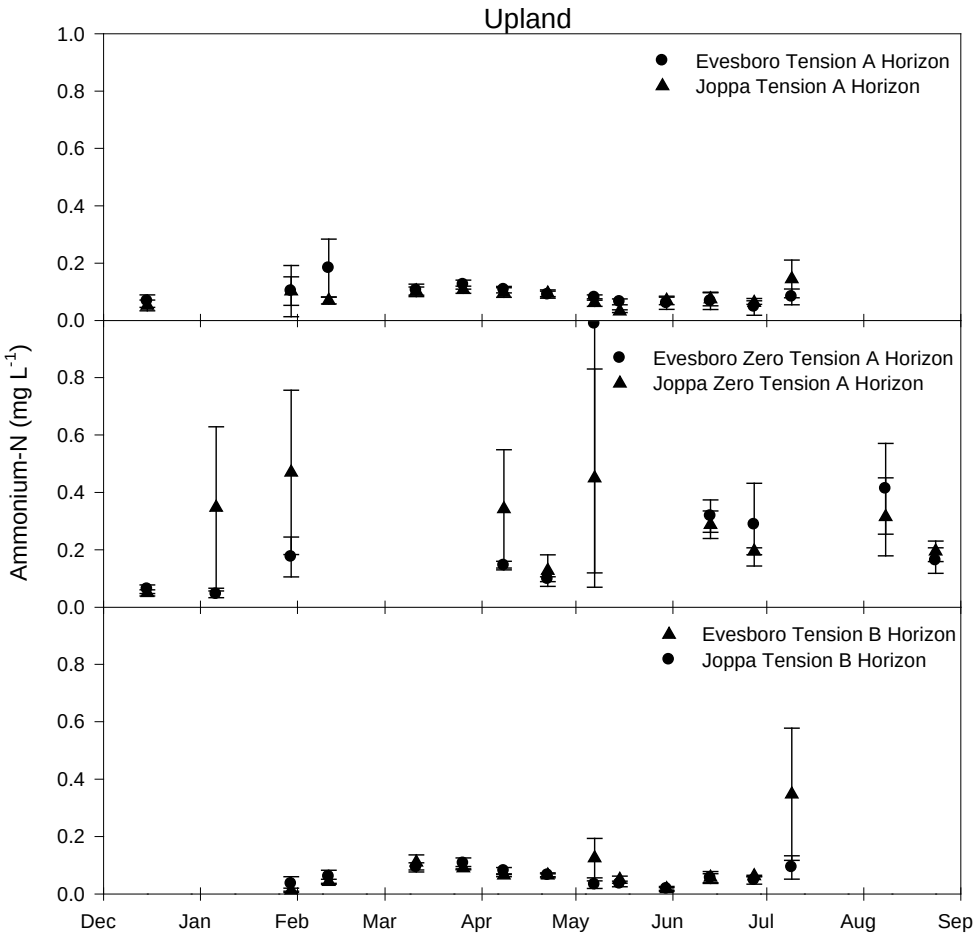

111

112 Figure S6. Temporal pattern of ammonium-N concentrations sampled in Entisol and Ultisol soil orders at
113 upland landscape locations with tension and zero tension lysimeters. For each soil order the mean and
114 standard error for is displayed for each sample date (N = 4).

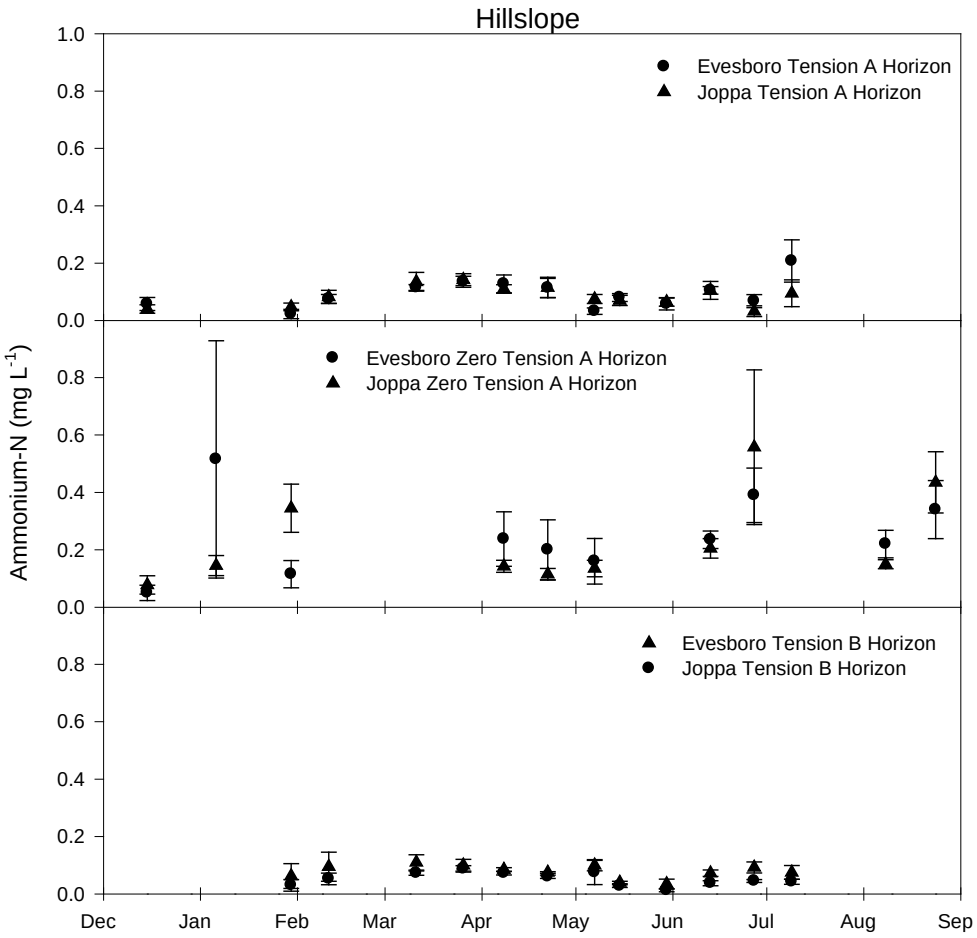

115

116 Figure S7. Temporal pattern of ammonium-N concentrations sampled in Entisol and Ultisol soil orders at
117 hillslope landscape locations with tension and zero tension lysimeters. For each soil order the mean and
118 standard error for is displayed for each sample date (N = 4).

119

120

121

122

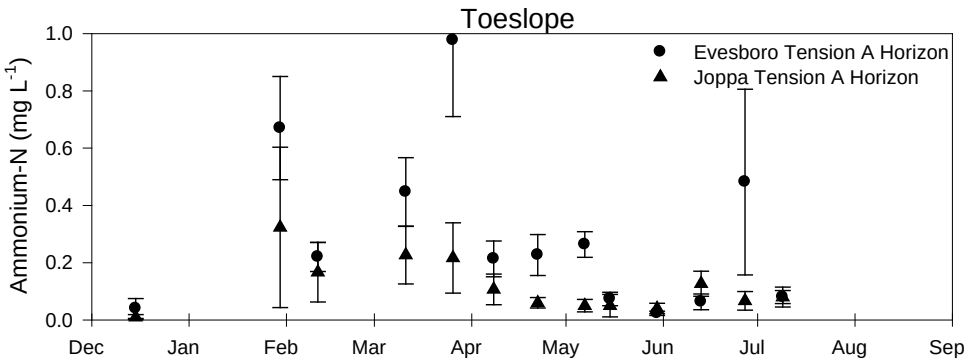

123

124 Figure S8. Temporal pattern of ammonium-N concentrations sampled in Entisol and Ultisol soil orders at
125 toeslope landscape locations with tension and zero tension lysimeters. For each soil order the mean
126 and standard error for is displayed for each sample date (N = 3).

127